

## An imaging proton spectrometer for short-pulse laser plasma experimentsa)

Hui Chen, A. U. Hazi, R. van Maren, S. N. Chen, J. Fuchs, M. Gauthier, S. Le Pape, J. R. Rygg, and R. Shepherd

Citation: [Review of Scientific Instruments](#) **81**, 10D314 (2010); doi: 10.1063/1.3483212

View online: <http://dx.doi.org/10.1063/1.3483212>

View Table of Contents: <http://scitation.aip.org/content/aip/journal/rsi/81/10?ver=pdfcov>

Published by the [AIP Publishing](#)

---

### Articles you may be interested in

[Time of flight emission spectroscopy of laser produced nickel plasma: Short-pulse and ultrafast excitations](#)  
J. Appl. Phys. **116**, 013301 (2014); 10.1063/1.4885760

[Investigation of longitudinal proton acceleration in exploded targets irradiated by intense short-pulse laser](#)  
Phys. Plasmas **21**, 013102 (2014); 10.1063/1.4853475

[Production of neutrons up to 18 MeV in high-intensity, short-pulse laser matter interactions](#)  
Phys. Plasmas **18**, 100703 (2011); 10.1063/1.3654040

[Designing and building an integrated target chamber system for high intensity short-pulse laser-target interaction experiments](#)  
Rev. Sci. Instrum. **74**, 1819 (2003); 10.1063/1.1538332

[Electric field detection in laser-plasma interaction experiments via the proton imaging technique](#)  
Phys. Plasmas **9**, 2214 (2002); 10.1063/1.1459457

---

The advertisement has a dark blue background with abstract circular patterns. On the left, there is a circular inset image showing a man with glasses and a beard, wearing a white lab coat, working with laboratory equipment. To the right of the image, the text reads: 'On the way to a graphene spin field effect transistor' in large white font, followed by 'by Prof. Barbaros and the Özyilmaz Group at National University of Singapore' in a smaller white font. In the top right corner, the Oxford Instruments logo is displayed with the tagline 'The Business of Science®'. At the bottom right, there is an orange rectangular button with the text 'Download a FREE application note' in white.

# An imaging proton spectrometer for short-pulse laser plasma experiments<sup>a)</sup>

Hui Chen,<sup>1,b)</sup> A. U. Hazi,<sup>1</sup> R. van Maren,<sup>1</sup> S. N. Chen,<sup>1</sup> J. Fuchs,<sup>2</sup> M. Gauthier,<sup>2</sup>  
S. Le Pape,<sup>1</sup> J. R. Rygg,<sup>1</sup> and R. Shepherd<sup>1</sup>

<sup>1</sup>Lawrence Livermore National Laboratory, Livermore, California 94551, USA

<sup>2</sup>LULI Ecole Polytechnique, 91128 Palaiseau Cedex, France

(Presented 17 May 2010; received 15 May 2010; accepted 26 July 2010;  
published online 19 October 2010)

The ultraintense short pulse laser pulses incident on solid targets can generate energetic protons. In addition to their potentially important applications such as in cancer treatments and proton fast ignition, these protons are essential to understand the complex physics of intense laser plasma interaction. To better characterize these laser-produced protons, we designed and constructed a novel spectrometer that will not only measure proton energy distribution with high resolution but also provide its angular characteristics. The information obtained from this spectrometer compliments those from commonly used diagnostics including radiochromic film packs, CR39 nuclear track detectors, and nonimaging magnetic spectrometers. The basic characterizations and sample data from this instrument are presented. © 2010 American Institute of Physics. [doi:[10.1063/1.3483212](https://doi.org/10.1063/1.3483212)]

## I. INTRODUCTION

Since the discovery<sup>1</sup> that intense short pulse lasers can accelerate protons to multi-MeV energies, a great deal of research has been performed to understand the process of laser-driven ion acceleration and the potential applications of the resulting ion beams.<sup>2</sup> This includes efforts to characterize the physics of acceleration, beam quality, laser to proton conversion efficiency, and scaling of the maximum proton energy with the laser parameters. Most of the previous research has focused on high-energy (greater than a few MeV) protons. This is partly because such protons are more relevant to applications such as the proton fast ignition research<sup>3</sup> and proton radiography of dense matter,<sup>4</sup> and partly because the radiochromic film (RCF) packs, which are covered with range filters, are often used to measure their energy and angular distributions. This diagnostic is not sensitive to low energy ions. The measurement and understanding of laser accelerated, low-energy (less than a few MeV) protons are particularly important due to the fact that these protons can efficiently heat (isochorically) solid samples to the “warm dense matter” regime. In addition, there is a great need for an experimental verification of the ion energy loss physics in plasma modeling codes, particularly in the moderately strongly coupled regime at low ion energies, where the stopping is more sensitive to the ion-plasma interaction physics.<sup>5</sup> To help answer these fundamental questions in the field of high energy density physics, we designed and constructed a high energy-resolution, imaging proton spectrometer (IPS) that covers the 0.05–5 MeV energy range. This paper de-

scribes the design principles and modeling analysis, as well as sample results from a laser-solid interaction experiment.

## II. SPECTROMETER DESCRIPTION

The design of the IPS is based on the fact that the laser accelerated protons are ballistic and behave as if they were emitted from a virtual point source.<sup>2</sup> Consequently, one may, in principle, trace their trajectories back to their origin (source), as illustrated in Fig. 1. The energy dispersion of the IPS is achieved by a pair of permanent magnets. The charged particles in the magnetic field will move along a curved trajectory (perpendicular to the field) with a Larmor radius determined by their kinetic energy and the charge to mass ratio. In the present design, the protons are detected near the sidewall of the spectrometer, in contrast to previous implementations, where they are detected at the back wall facing the entrance aperture.<sup>6</sup>

In principle, the IPS can be used to measure the energy spectrum of fast electrons as well. However, electron measurement is only secondary in the present instrument since the magnetic field strength was chosen to optimize the proton measurement. The actual imaging and dispersion properties of the IPS are not simple due to the magnetic structure of the spectrometer, as will be discussed below. The energy coverage of the spectrometer is between 50 keV and ~5 MeV. We chose the photostimulable image plates (IPs) as the proton detector, since they can provide a large dynamic range and high sensitivity to energetic protons.<sup>6,7</sup> The spectrometer is designed to be compact with approximate dimensions of 13 cm × 8.5 cm × 19 cm. This is particularly important because usually only limited amount of space is available for an individual diagnostic in vacuum chambers used in intense laser-solid interaction experiments. To cut down the background noise from high energy photons, the whole spectrom-

<sup>a)</sup> Contributed paper, published as part of the Proceedings of the 18th Topical Conference on High-Temperature Plasma Diagnostics, Wildwood, New Jersey, May 2010.

<sup>b)</sup> Author to whom correspondence should be addressed. Electronic mail: [chen33@llnl.gov](mailto:chen33@llnl.gov).

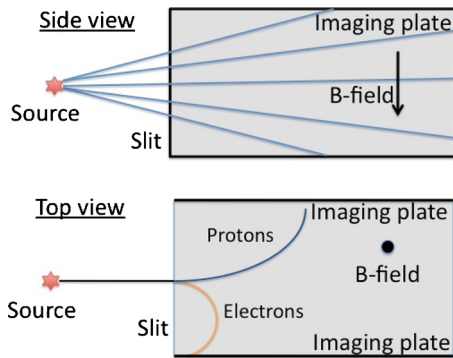


FIG. 1. (Color online) The schematic of the IPS. Top (side view): the imaging property based on straight trajectories of the protons in the  $xy$ -plane. Bottom (top view): the energy dispersion of the IPS.

eter is shielded in the front with “heavy” metal in combination with low  $Z$  plastic. The body is fabricated from 0.5-inch-thick steel.

### A. Energy dispersion

The dispersion (proton energy versus position on the image plate detector) of the spectrometer was determined using a combination of measurements and simulations of the magnetic field inside the instrument. A Faraday probe was used to map the  $y$ -component of the magnetic field (the component parallel to the slit) as a function of position in a plane defined by the slit and the long-axis of the spectrometer. For these measurements, the slit assembly was removed, and the probe was inserted through a slot in the front steel plate. The accuracy of the field mapping was limited by the flexing of the thin arm holding the probe at long extensions beyond the front plate. The simulations of the magnetic field were performed using the two-dimensional finite-element magnetic code FEMM (V4.2).<sup>8</sup> For these calculations, the dimensions of the critical components of the spectrometer were imported directly from the CAD drawing of the entire instrument. The magnetic properties of the various components were taken from the built-in materials library in FEMM. The 2D mesh was chosen sufficiently dense ( $\sim 60$  K nodes and  $\sim 115$  K elements) and so that the calculated  $B$ -field values were stable within a few percent.

Because of the relatively large separation of the magnets required for spatial imaging, there is a significant spatial variation of the magnetic field, with  $B_y$  increasing by approximately a factor of 2 from midway between the magnets to locations adjacent to the magnets, as shown in Fig. 2. Along the direction perpendicular to the slit ( $z$ -axis),  $B_y$  approaches zero at the sidewalls of the spectrometer. The dispersion along the centerline of the image plate was determined semianalytically using the calculated values of  $B_y(z)$  and the distance between the slit and the image plate. The absolute value of the magnetic field (and the dispersion at a single energy) was calibrated by measuring the proton spectrum with an image plate (type BAS-MS-2040), which has a  $9\text{ }\mu\text{m}$  polyethylene terephthalate (PET) layer on the top of the active layer.<sup>7</sup> The PET layer acts as a range filter and results in a sharp, low-energy cutoff in the spectrum.<sup>9</sup> We used the stopping power of PET,<sup>10</sup> along with the calculated

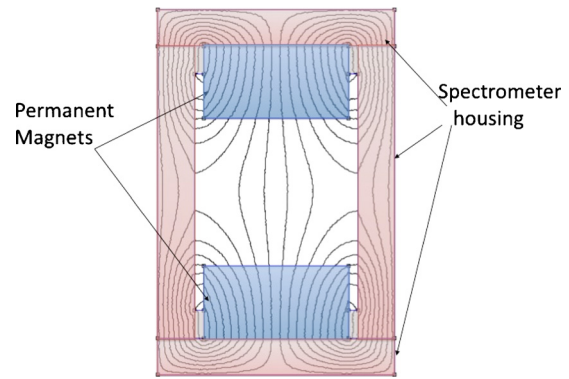


FIG. 2. (Color online) The magnetic structure of the IPS (front view) modeled by the FEMM code. The magnetic field is not uniform; the closer it is to the magnets, the stronger is the magnetic field.

angle of incidence of the protons on the image plate at the spatial location of the cutoff to determine the proton energy corresponding to that location. The energy resolving power ( $E/dE$ ) of the IPS is about 250 at 0.5 MeV and  $\sim 350$  at 2 MeV. This is substantially higher than that can be achieved with RCF packs.

The dispersion at all points on the image plane can be constructed using a three-dimensional code. However, it can also be derived experimentally. Shown below is the image of a measured spectrum, superimposed with the fitted 2D dispersion contours, where the dispersion along the centerline is constrained by the calibrated, analytical dispersion curve discussed above.

### B. Imaging property

The imaging capability of the spectrometer is achieved by using a long ( $\sim 5$  cm), narrow slit, parallel to the magnetic field, through which the protons enter the interior of the instrument (Fig. 3). The width of the slit ( $w_s$ ) is adjustable and is normally set between 50 and  $100\text{ }\mu\text{m}$  to maintain good energy resolution. The narrow slit geometrically constrains the position and velocity of the entrant protons in the

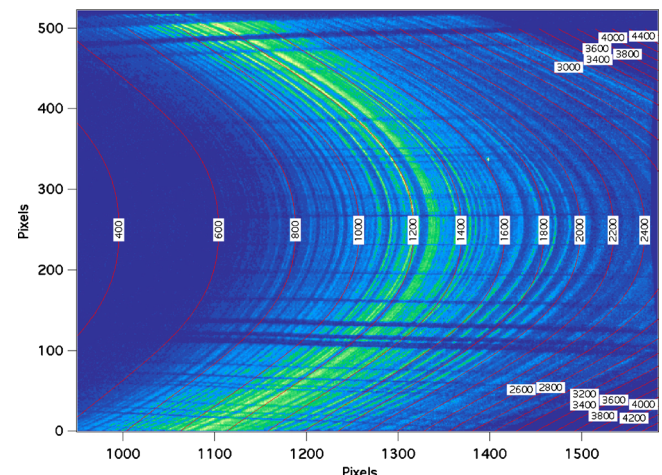


FIG. 3. (Color online) The isoenergy contours of the IPS dispersion superimposed on a measured spectrum. The numbers listed are the energy in the unit of keV. The image is about 5 cm wide and 15 cm long. The pixel size is  $100\text{ }\mu\text{m} \times 100\text{ }\mu\text{m}$ .



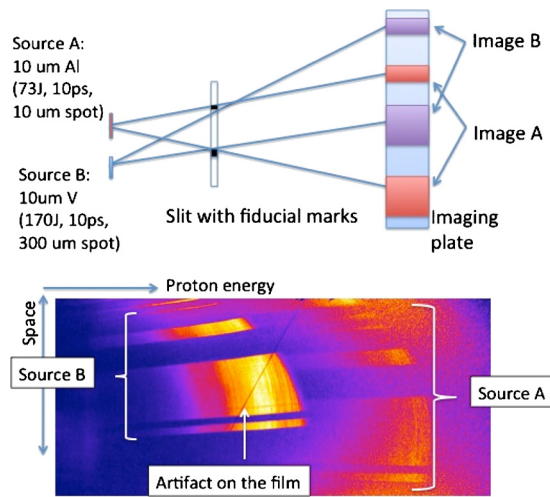


FIG. 4. (Color online) The schematics of the experimental setup (top) and the resulting spatially resolved proton image (bottom). The laser and target condition for the two sources are noted. Two proton sources are clearly imaged on the energy dispersing image plane with the dark gaps being caused by the C-foils mounted across the slit. The thin slanted line on the image is caused by an artifact (scratch) on the image plate and is not related to the proton sources.

$z$ -direction, perpendicular to the slit. Therefore, one needs to consider only the proton's entry point along the slit ( $y_s$ ) and its two velocity components ( $v_x$  and  $v_y$ ). For a diverging laminar beam emanating from a point source,  $y_s$  is related to the velocity components through the relation:  $(y_s - y_0)/L = v_y/v_x$ , where  $y_0$  is the vertical position of the source point relative to the centerline of the IPS and  $L$  is the distance (along  $x$ ) between the source and the slit.  $L$  and  $y_0$  are the same for all protons in the beam regardless of their angle of incidence. By using the fiducial markers (e.g., metal wires or strips) mounted across the slit, one can identify those protons that entered the spectrometer at  $y_s$ . This allows one to reconstruct the energy and angle of these protons from their landing position ( $x, y$ ) on the image plate detector. Tracing the trajectories of these protons back to the source provides information about the location of the virtual point source, and the position and angle of emission of the protons at the target. This is the "imaging" capability of the instrument.<sup>11</sup> For

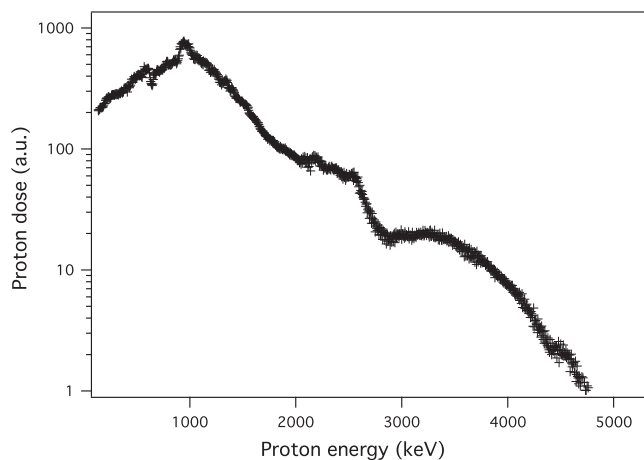


FIG. 5. Sample proton energy spectrum taken by the IPS from a short-pulse laser experiment.

typical experimental geometries ( $L=10\text{--}20\text{ cm}$ ) and  $w_s=100\text{ }\mu\text{m}$ , the field of view of the IPS is a few millimeters in the direction perpendicular to the slit, and a few centimeters parallel to the slit. In the direction parallel to the slit, the acceptance angle of the IPS is about  $\pm 5^\circ$ , assuming  $y_0 \approx 0$  and  $L=12\text{ cm}$ .

### III. TEST OF THE IPS IN A LASER EXPERIMENT

We tested the imaging property as well as the energy dispersion characteristic of the IPS on the Titan laser at the Jupiter Laser Facility at the Lawrence Livermore National Laboratory.<sup>12</sup> Figure 4 shows the experimental setup and a sample result illustrating the imaging capability of the IPS. Several carbon foils (with various thickness and widths) were mounted across the slit of the IPS at different positions. These foils served as fiducial markers by creating shadows on the image plate by stopping protons coming from the source at certain angles. In this experiment, two separate laser pulses from Titan illuminated two different targets creating two spatially separated proton sources (A and B). Source A was made by irradiating a  $10\text{-}\mu\text{m}$ -thick Al foil with 73 J laser energy in 10 ps, with a  $\sim 10\text{ }\mu\text{m}$  diameter focal spot. The laser intensity was about  $5 \times 10^{18}\text{ W cm}^{-2}$  corresponding to maximum proton energy of 1–2 MeV,<sup>13</sup> as shown in Fig. 4. The second source (B) was made by a lower intensity but higher energy laser pulse (170 J, 10 ps with  $300\text{ }\mu\text{m}$  diameter focal spot, which is equivalent to  $1 \times 10^{16}\text{ W cm}^{-2}$ ) irradiating a  $10\text{-}\mu\text{m}$ -thick vanadium target. The measured maximum proton energy for source B is about 300 keV. The spacing of the two focal spots was about  $700\text{ }\mu\text{m}$ . The two proton sources are well resolved by the IPS, as shown in Fig. 4.

Figure 5 shows a sample proton energy spectrum obtained with the IPS in a different experiment. The spectrum has its maximum near a proton energy of 100 keV, and then decreases quasiexponentially at higher energies.<sup>2</sup> The physics behind the structure in the measured spectrum is to be studied in the future.

### IV. SUMMARY AND FUTURE WORK

In this paper we, describe the design and test of a new imaging proton spectrometer. This instrument features physical compactness, high resolving power for the proton energy, and the ability to measure the emission characteristics of the proton source. We expect it will be useful in measuring the source structure and energy spectrum of low energy protons produced in short pulse laser-solid interaction experiments. Future work on the IPS will include absolute calibration of the image plate detection system in the current geometry, so that the measured IP counts per pixel can be converted to number of protons. Calibration of the energy dispersion at multiple energies is also desirable to improve the accuracy of the present dispersion curve based on simulations and measurement with a range filter at a single energy.

### ACKNOWLEDGMENTS

This work was performed under the auspices of the U.S. Department of Energy by Lawrence Livermore National

Laboratory under Contract No. DE-AC52-07NA27344 as part of the Cimarron project funded by LDRD-09SI11.

- <sup>1</sup>R. A. Snavely, M. H. Key, S. P. Hatchett *et al.*, *Phys. Rev. Lett.* **85**, 2945 (2000).
- <sup>2</sup>For a comprehensive review, see M. Borghesi, J. Fuchs, S. V. Bulanov *et al.*, *Fusion Sci. Technol.* **49**, 412 (2006).
- <sup>3</sup>M. Roth, T. E. Cowan, M. H. Key *et al.*, *Phys. Rev. Lett.* **86**, 436 (2001); M. Temporal, J. J. Honrubia, and S. Atzeni, *Phys. Plasmas* **9**, 3098 (2002).
- <sup>4</sup>See Sec. IVA in Ref. 2.
- <sup>5</sup>V. Fortov, I. Iakubov, and A. Khrapak, *Physics of Strongly Coupled Plasma* (Oxford University Press, Oxford, UK, 2006).
- <sup>6</sup>A. Mančić, J. Fuchs, P. Antici *et al.*, *Rev. Sci. Instrum.* **79**, 073301 (2008).
- <sup>7</sup>The photostimulable image plates are also called storage phosphor screens and are now available from GE Healthcare, Piscataway, N.J., USA.

For product information, see <http://www.gelifesciences.com/aptrix/upp01077.nsf/Content/Products?OpenDocument&parentid=957136&moduleid=163735&zone=>.

- <sup>8</sup>See: <http://femm.foster-miller.com> for a description of the FEMM code; dmeecker@ieee.org.
- <sup>9</sup>P. Antici, Ph.D. thesis, Ecole Polytechnique, France, 2007, Sec. A5.1.
- <sup>10</sup>SRIM-2008; J. F. Ziegler, J. P. Biersack, and U. Littmark, *The Stopping and Range of Ions in Solids* (Pergamon, New York, 1985).
- <sup>11</sup>After the submission of this paper, we became aware that the work of S. Ter-Avetisyan, M. Schnürer, P. V. Nickles, W. Sandner, M. Borghesi, T. Nakamura, and K. Mima, *Phys. Plasmas* **17**, 063101 (2010), in which the authors used a similar instrument to tomographically reconstruct the emission characteristics of a laser-driven proton source.
- <sup>12</sup>See: <https://jlf.llnl.gov> for a description of the Titan laser.
- <sup>13</sup>See Fig. 9 in Ref. 2.